Influence of paste thickness on coated aggregates on properties of high-density sulphoaluminate cement concrete

Sun Keke[1], Zhou Xiangming[2], Gong Chenchen[1], Ding Yanyu[1], Lu Lingchao[1]

1. Shandong Provincial Key Laboratory of Preparation and Measurement of Building Materials, Jinan, Shandong, China, 250022
2. Department of Mechanical, Aerospace and Civil Engineering, Brunel University London, Uxbridge, Middlesex UB8 3PH, United Kingdom

Abstract: An improved method for the densified mixture design algorithm and Fuller curve were used to design high-density sulphoaluminate cement concrete (HDSC). The performance of HDSC is significantly influenced by the paste thickness on the coated aggregates. Sulphoaluminate cement concrete mixtures containing aggregates coated with 3 different paste thickness of t=10μm, 20μm, and 30μm and water-binder ratios (W/B) of 0.25, 0.30 and 0.35 were prepared. The results of experiments show that paste thickness on the coated aggregates significantly influences the mechanical properties and durability of HDSC. With the increase of paste thickness, the compressive strength is increased, but the electrical resistivity is decreased, particularly at the early ages of 1 and 3 days. The sulfate corrosion resistance coefficients of HDSC are larger than 1.0, the total porosity can be less than 7%, and the micropore (i.e. with pore size less than 20nm) can be larger than 70%.

Keywords: sulphoaluminate cement concrete; Fuller curve; densified mixture design algorithm; coating thickness; durability

1. Introduction

Sulphoaluminate cement is a type of “low energy” cement compared to Portland cement [1], possessing advantageous properties such as high early-age compressive strength, short setting time and shrinkage compensation and it is typically used in the

marine engineering field [2-4]. However, as a special type of cement, the mechanical properties and durability [5-6] of sulphoaluminate cement concrete (SACC) has not been well studied. Under harsh environments, the harmful external ions and water can easily permeate into the concrete interior, destroying its structure and shorten its service life. However, a compact concrete structure can lead to improved strength and durability. The importance of pore structure and its impact on durability has been highlighted in numerous studies [7]. Many researchers also found that the concrete pore structure improved the interfacial transition zone (ITZ) and dominated engineering properties, such as strength and durability [8-9]. For such reasons, high-density concrete has been widely used to achieve outstandingly durable concrete structures.

However, it must be noted that little work has been conducted on SACC mixture design as a high-density concrete. Therefore, the major work required is designing an appropriate mix proportion to produce the high-density sulphoaluminate cement concretes (HDSCs). The densified mixture design algorithm (DMDA) is derived from the maximum density theory and excess paste theory, proposed by Hwang et al. [10-12]. This method is based on the hypothesis that the physical properties can be optimized when the packing density is high. The major difference from the other mixture design algorithms is that instead of partial replacement of cement, DMDA incorporated the use of fly ash to fill the void between aggregates and hence increase the density of the aggregate system. In such a way, the cement paste content can be reduced without affecting the other properties such as workability, and strength [13]. Lots of research [13-16] shows that it is feasible to produce the eco-friendly construction bricks, lightweight concrete, high-performance concrete and self-compacting concrete using the DMDA method with the incorporation of an admixture, such as fly ash or slag powder. However, to simplify the derivation, it is necessary to assume that the aggregate is spherical, which is physically very hard to achieve and thus gives rise to errors.

In additional, it is commonly thought that the cement paste volume is a key factor in achieving a desirable concrete workability and durability [17-19]. A work studied

the effect of cement content on transport processes important to the durability of concrete structures, such as electrical conduction and chloride diffusion. It was found that the resistance to transport reduced as cement content was increased [20]. Hwang et al. proposed a particular DMDA, in which the concept and formula of the paste thickness on coated aggregates were introduced. A complete and precise formula to estimate the optimum coating thickness on the aggregates was derived to ensure the use of sufficient coating paste and a dense concrete structure is obtained [21]. Kolias and Georgiou studied the effect of paste volume and of water content on capillary absorption and strength on concrete mixes. It is found that strength increases and capillary absorption decreases when the volume of the water or the volume of the paste decreases [22]. Chen et al. demonstrated that the paste thickness on the coated aggregates has a positive effect on the slump flow, concluding that a thickness of $42\mu m$ produced self-compacting concrete which flowed to a diameter of $680mm$ [23]. Last but no least, using less cement reduces energy consumption and CO_2 emissions associated with its production process.

In this paper, an improved DMDA method is developed to simplify the calculation process. Introducing the assumption that the aggregates are square and spherical in shape allows a more accurate engineering design requirement to prepare HDSC. The Fuller curve was used to calculate the aggregate gradation, and the sieve analysis was used to calculate the specific surface area of aggregates. Sulphoaluminate cement, replaced by approximately 5% superfine slag powder, and 10% fly ash, both by weight, was used as the cementitious materials for preparing the HDSC and the improved DMDA calculated the dosage of cementitious material. Finally, the effects of paste thickness around the aggregates on mechanical and durability properties of HDSC were investigated.

2. Raw materials and methods

2.1 Sulphoaluminate cement and admixtures

Sulphoaluminate cement of strength class 42.5, fly ash and slag powder were imported from mainland China. The chemical compositions of the sulphoaluminate

cement, fly ash and slag powder are shown in Table 1. The average particle size of fly ash and slag powder are 14.34μm and 2.98μm, respectively. The superplasticizer (SP) used was a polycarboxylate polymer, and its water-reducing capacity in SACC was over 20%.

Table 1 Chemical composition of raw materials (wt.%)

Materials	SiO_2	Al_2O_3	CaO	MgO	Fe_2O_3	Other	Loss
Sulphoaluminate cement	11.41	27.87	43.86	-	2.59	13.11	1.16
Fly ash	50.55	29.01	6.00	5.44	-	4.12	2.08
Slag powder	29.46	17.44	34.71	11.02	-	0.3	0.30

2.2 Aggregates

River sand (0.075-2.36mm in size) was used as fine aggregates with an apparent density of 2710kg/m^3, and crushed natural stone (2.36-16mm in size) was applied as a coarse aggregate with an apparent density of 2740kg/m^3. The aggregate mix proportions were also key to improving the packing density of concrete [24]. Fuller curve was based on defining conventional concrete dosages by selecting coarse and fine aggregate proportions according to the adjustment within the standard curve that allows for the maximum compaction of granular elements, which is the method that corresponds to the Gessner parabola [25]. Since the Fuller curve was proposed, it has been used for designing concrete mixes for many applications, particularly for those of high-density and high-performance concrete [26-28]. The Fuller curve is a series of curves, widely used for the optimization of concrete aggregates, and expressed as:

$$U(j) = 100 \times (j/D_{max})^h \quad (1)$$

where *U(j)* is the total volume percent of particles passing through a sieve, (*%*); D_{max} is the maximal size of the aggregate, (*mm*); *j* is the diameter of the particular sieve, (*mm*); and *h* is the exponent of the equation.

The value for *h*, which varies from 0.33 to 0.45, was selected as 0.33 [26, 29] in this study. The mass ratios of aggregates of different particle size are given in Table 2, calculated using Equation (1).

Table 2 Mass ratios of aggregates with different gradations (*wt.%*)

Grain size *(mm)*	0.075-0.15	0.15-0.30	0.30-0.60	0.6-1.18	1.18-2.36	2.36-4.75	4.75-9.50	9.50-16.0
wt.%	0.13	0.17	0.21	0.27	0.35	0.47	0.43	0.39

2.3 Methods

2.3.1 Concrete samples preparation

The concrete samples were made according to Chinese national standard for testing fresh concrete GB/T50080-2002 [30] (equivalent to ASTM C192M-02). All concrete samples, measured $100mm \times 100mm \times 100mm$, were cured at 20±2°C in molds for the first 24h, then demoulded and cured in an environment of 20±2°C and at 95±5% RH until the day of testing.

2.3.2 Compressive strength test

The compressive strength test of concrete was carried out according to the Chinese National Standard for testing mechanical properties of concrete GB/T 50081-2002 [31] (equivalent to ASTM C39). The compressive strength of concrete was evaluated for the ages of 1, 3 and 28 days at a loading rate of 0.5*MPa/s* as per GB/T 50081-2002.

2.3.3 Electrical resistance test

In this study, the concrete was mixed with a water-binder ratio (0.25, 0.30 and 0.35) and cast into $100mm^3$ cubes for the electrical resistance test. The negative and positive copper electrodes were placed parallel to each other inside the cubic concrete samples, and the average testing results of the three samples were taken as the representative value. The schematic diagram of the concrete specimen prepared for electrical resistivity measurement is shown in Fig.1.

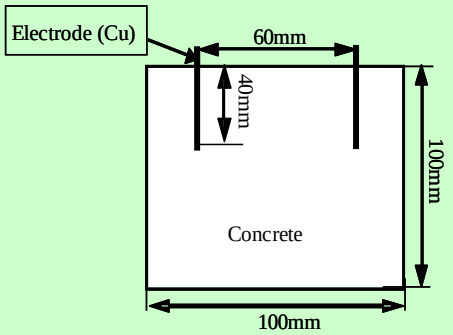

Fig.1 Schematic diagram for concrete electrical resistivity measurement

2.3.4 Sulfate attack resistance

The resistance of concrete to sulfate attack was conducted according to Chinese national standard for testing durability of concrete GB/T 50082-2009 [32] (equivalent to ASTM C 1012). The solution was made by dissolving reagent grade sodium sulfate (Na_2SO_4) in deionized water and contained a final SO_4^{2-} concentration of 33,800*ppm* (i.e. 5% Na_2SO_4). All specimens were stored in plastic containers having the solution with ample space between them. The containers with the specimens were stored in a constant temperature (20±1℃) room and the solutions were replenished periodically once a week to remain the designated concentration. Other control concrete cubes were kept in deionized water as well. The degree of sulfate attack was evaluated by measuring the compressive strength of concrete samples at 28 days, and the ratio of compressive strength was calculated by Equation (2) as follows:

$$K_f = \frac{f_{cn}}{f_{c0}} \tag{2}$$

where, K_f is the compressive strength ratio, (%); f_{c0} is the average compressive strength (in *MPa*) of the control concrete cubes cured for 28 days in deionized water; and f_{cn} is the average compressive strength (in *MPa*) of three concrete cubes immersed in 5% sodium sulfate solution for 28 days.

3. Dosage of cementitious materials

3.1 Packing model of concrete

According to classical concrete mixture proportion design, the aggregates are considered the main skeleton of concrete and the paste requirements for workable

concrete are determined by the aggregate gradation. Effective packing can be attained by selecting accurate proportions of small size particles to fill in the voids between the bigger particles. The Fuller model is considered to be an effective method for preparing high-density concrete by adjusting the particle size for optimum aggregate packing [33-34]. The concrete model structure is shown in Fig.2. In the diagram, the aggregates, shown in black, are representing the concrete skeleton, the paste coating them is shown in gray, and the white area among the aggregates are the voids.

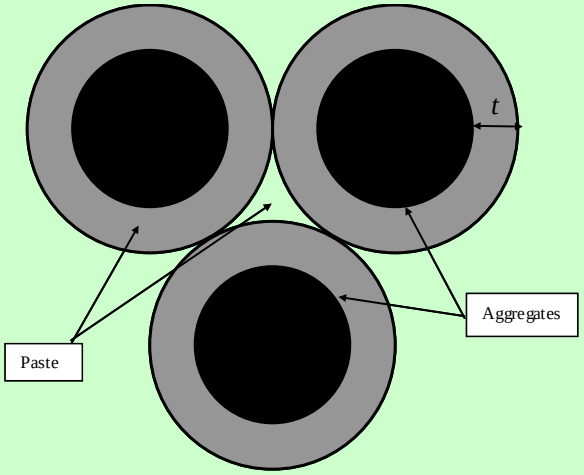

Fig.2 Diagrammatic model of aggregates and paste in concrete.

3.2 Calculation process of cement paste dosage

(1) The calculation process of the specific surface area of aggregates

The aggregate specific surface area calculation process was simplified by assuming all aggregates to be either spherical or square. The volume of each particle is shown in the Equation (3):

Spherical: $\frac{m}{\rho} = V = \frac{4}{3}\pi\left(\frac{D}{2}\right)^3 = \frac{1}{6}D \cdot \pi D^2 = \frac{1}{6}D \cdot A$

Square: $\frac{m}{\rho} = V = D^3 = \frac{1}{6}D \cdot 6D^2 = \frac{1}{6}D \cdot A$ (3)

Then, according to the definition of the specific surface area with the combination of Equation (3), Equation (4) could be derived as following.

$$\frac{n \cdot A}{n \cdot m} = \frac{A}{D \cdot A \cdot \rho} \cdot 6 = \frac{6}{D \cdot \rho} \quad (4)$$

where m is the mass of each aggregate particle, (in g); ρ is the apparent density of aggregates, (in kg/m^3); V is the volume of each aggregate particle, (in cm^3); D is the particle size of aggregate, (in mm); A is the specific surface area of each aggregate particle, (in cm^2); and n is the number of aggregate particles.

The aggregate is of varying particle size, so the specific surface area of the aggregates could be achieved according to Equation (5):

$$A_s = \frac{\sum_i \left(\frac{6000}{D_i \cdot \rho} m_i \right)}{M} = \frac{6000}{\rho} \cdot \sum_i \left(\frac{K_i}{D_i} \right) \quad (5)$$

where A_s is the specific surface area of aggregates, (in m^2/kg); D_i is the intermediate particle size of each aggregate gradation, (in mm); M is the total mass of aggregates, (in kg); m_i is the total mass of each aggregate gradation, (in kg); and K_i is the mass fraction of each aggregate gradations, i.e. m_i/M in %. Based on calculation, the specific surface area of aggregates with different gradations is shown in Table 3.

Table 3 Specific surface area of aggregates

Gradation（mm）	D_i (mm)	K_i（%）	A_s（m^2/kg）
0.075-0.15	0.11	4.5	
0.15-0.30	0.23	6.0	
0.30-0.60	0.45	7.8	5.73
0.60-1.18	0.92	10.0	
1.18-2.36	1.77	12.7	
2.36-4.75	1.20	17.1	
4.75-9.50	7.13	21.7	0.71
9.50-16.0	12.75	20.4	

(2) The calculation process of the total paste volume

Supposing that the average paste thickness of coated aggregates was termed as t (in μm), the dosage of paste was calculated using Equations (6) and (7):

$$V = \mathrm{t} \cdot (M_s A_s + M_G A_G) + V_b \quad (6)$$

where V is the unit volume of the paste, (in m^3); t is the average paste thickness on the coated aggregates, (in μm); M_S is the dosage of fine aggregates, (in kg); M_G is the dosage of coarse aggregates, (in kg); A_S is the specific surface area of fine aggregates, (in m^2/kg); A_G is the specific surface area of coarse aggregates, (in m^2/kg); and V_b is the volume of paste required to fill the pores between the aggregates, (in m^3);

$$V_b = \frac{M_S}{\rho_S} \cdot P_S = \frac{M_S}{\rho_S} \cdot (1 - \frac{\rho_S}{\rho_S'}) \quad (7)$$

where ρ_S is the packing density of fine aggregates, (in kg/m^3); ρ_S' is the apparent density of fine aggregates, (in kg/m^3); and P_S is the porosity of fine aggregates, (in %).

Based on the concept of particle packing, well-graded aggregates have fewer voids among particles than poorly graded aggregates requiring less cement paste to fill the voids. Thus, the additional amount of cement paste remaining can be used to coat the aggregate particles and improve the concrete fluidity. For the same reason, an increase in the volume fraction of aggregates generally results in a reduced concrete fluidity. A high-density concrete with desirable workability is obtained when a suitable amount of cement paste is provided to fill the spaces among the aggregates. The dosages of cementitious materials with coating thickness of t=10μm, 20μm and 30μm [35-36] are shown in Table 4, respectively. The water-binder ratio was fixed at 0.25, 0.30 and 0.35 after a series of trial mixes, satisfying the requirements of concrete with a slump of 250±10*mm*, respectively.

Table 4 Water-binder ratio and dosages of cementitious material in HDSCs

No.	Water-Binder ratio	Coating thickness	Cement *(kg/m³)*	FA *(kg/m³)*	SS *(kg/m³)*	SP *(kg/m³)*
A1	0.25	t=10μm	324	74	39	4.37
B1		t=20μm	382	88	47	5.17
C1		t=30μm	441	101	54	5.96
A2	0.30	t=10μm	299	69	36	4.04
B2		t=20μm	353	81	43	4.77
C2		t=30μm	407	94	50	5.51
A3	0.35	t=10μm	278	64	34	3.76
B3		t=20μm	328	75	40	4.43
C3		t=30μm	378	87	46	5.11

4. Results and Discussions on Properties of HDSC

4.1 Compressive strength

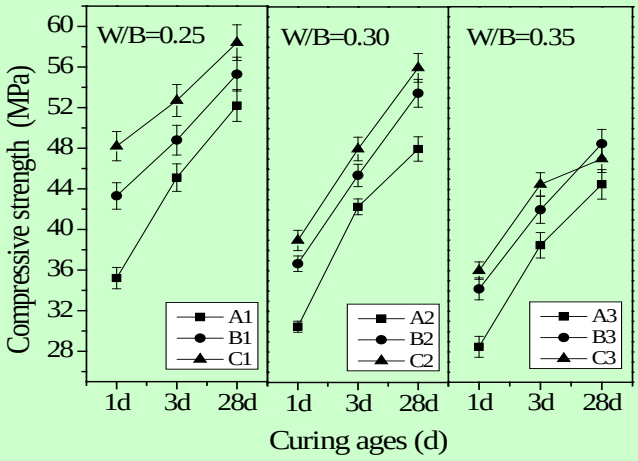

Fig.3 Relationship between pastes thickness on the coated aggregates and compressive strength of HDSCs

Fig.3 shows the compressive strength of HDSC at different water-binder ratios. It can be found that for all three different water-binder ratios, the compressive strength of concrete increased with the increase of paste thickness on the coated aggregates, especially at the early age of 1 and 3 days. Compared with A1, the compressive strength of B1 increased 23%, 8% and 6%, and C1 increased 37%, 17% and 12% at the curing ages of 1, 3 and 28 days respectively. The reason is that the sulphoaluminate cement typically attains high early age strength, which is a result of the cement hydration and increases the interfacial bonds in concrete. Table 4 shows that the cement dosage increased for the same coating thickness.

At a water-binder ratio of 0.30 and 0.35, concrete samples at 28 days attained very simmilar compressive strengths for aggregates with a coating thickness of 20μm and 30μm. Although the general trend shows the concrete compressive strength increasing with increase of the paste thickness on the coated aggregates, the compressive strength of B2 is close to that of C2 and the compressive strength of B3 is higher than that of C3. The reason can be mainly attributed to the paste thickness on the coated aggregates which improved the structure of the interface transition zone (ITZ) between cement paste and the aggregates. With the decrease of the coating thickness, the space of crystal growth decreases, and the gel could improve the cohesive strength and degree of density [37-38]. The SEM images of concrete A3, B3 and C3 are shown in Fig.4, and it can be seen clearly that the hardened cement paste has plenty of gel (C-S-H gel and $Al(OH)_3$ gel), fine AFt and little $Ca(OH)_2$. The hydration of sulphoaluminate

cement can produce plenty of gel and AFt in B3, leading to a more compacted ITZ compared with A3 and C3.

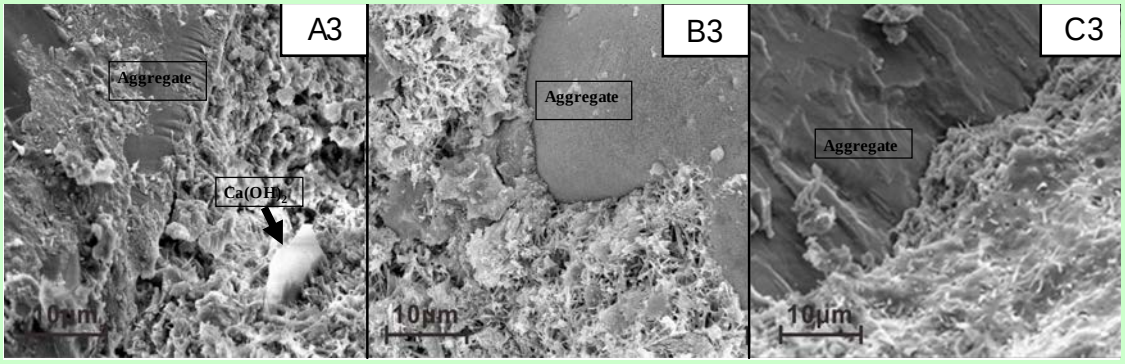

Fig.4 SEM images of interfacial transition zone (ITZ) for HDSCs at 28 days

4.2 Electrical resistivity

Several studies [39-40] consider electrical resistivity of concrete is an important factor that indicates the permeability of concrete to aggressive agents such as chloride and carbon dioxide, because electrical resistivity has a strong correlation with the concrete microstructure. The electrical resistivity was decided by the pore solution, which provided a path of conductive ions. This improved conductive performance, and accelerated the corrosion of concrete cubes [41-42].

The electrical resistivity results for HDSCs are shown in Fig.5. The electrical resistivity of all the samples increased with the rise of the curing age, particularly at the ages of 1 and 3 days. This can simply be explained by the fact that sulphoaluminate cement has the characteristic of rapid hydration and hardening, and the porosity of hardened cement paste is higher than that of the aggregates. With the increase of paste coating thickness on the coated aggregates, the electrical resistivity of HDSCs decreased at all three water-binder ratios. The electrical resistivity of A1 was 44%, 33% and 13% higher than that of C1 at the ages of 1, 3 and 28 days, respectively. Sample A2 was 42%, 35% and 23% higher than that of the sample C2 at the ages of 1d, 3 and 28 days, respectively. From Table 4, the dosage of cement increased with the increase of the paste thickness on the coated aggregates. So porosity of concrete relatively increased with the increase of the sulphoaluminate cement dosage at the same water-binder ratio.

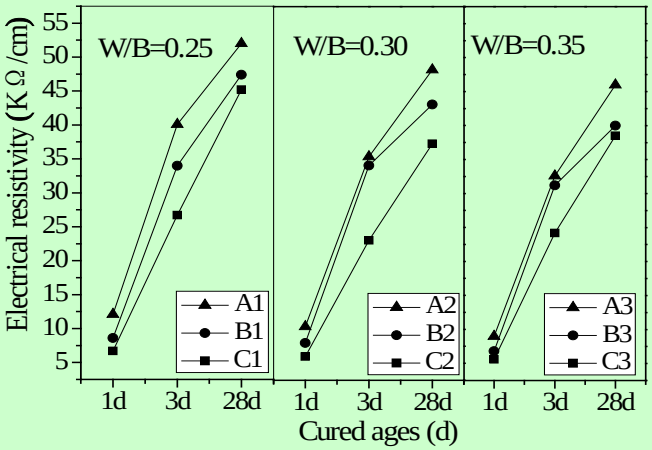

Fig.5 Effect of the paste thickness on the coated aggregates on electrical resistivity of HDSC

4.3 Sulfate attack resistance

The coefficient of sulfate attack resistance is a key parameter in measuring the durability of concrete hence the resistance coefficients of HDSCs were calculated using Equation (2). The coefficients of sulfate attack resistance at the curing age of 28 days are shown in Fig.6. The sulfate attack resistance coefficients of HDSCs were higher than 1.0, which means that the compressive strength of concrete samples cured in the 5% Na_2SO_4 solutions are higher than of those cured in the water at 28 days, indicating that former samples have much better capability of resisting sulfate attack. With the increase of paste thickness on the coated aggregates, the sulfate attack resistance coefficients decreased evidently at the same water-binder ratio. The coefficient of A1 was 10% higher than that of C1, and A3 was 6% higher than that of C3. Sulfate attack resistance is a very important property of concrete and many studies have found that the use of an excessive amount of cement, or too much water, can result in high permeability which has a negative effect on the durability [14, 15, 43]. When the amount of paste thickness on the coated aggregates was appropriate, the structure of concrete could reach up to the close packing. Using too little paste was not enough to fill the voids between the aggregates and too much paste would break the close packing structure, which can be used to explain the reduced sulfate attack resistance of C3. Therefore, the proper dosage of cement can also be used to produce

HDSCs with excellent mechanical properties and elevated resistance to sulfate attack.

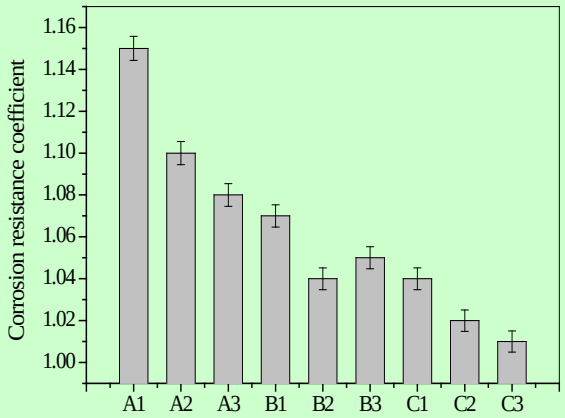

Fig.6 Sulfate attack resistance of HDSCs at a curing age of 28 days

4.4 Pore structure of HDSCs

The pore structure of A1, B1 and C1 at a curing age of 28 days is shown in Figure 7, Figure 8 and Table 5. Figures 7 and 8 showed that the number of micropore (less than 20nm) and macropore (more than 200*nm*) was more than 70% and less than 10% respectively. The cumulative volume of pores in A1 was much more than that in C1, and the volume of micropore of the former was lower than that of the latter. These pore structure results are in accordance with the results of electrical resistivity (t=10μm) in Fig.5 and sulfate corrosion resistance (t=10μm) in Fig.6.

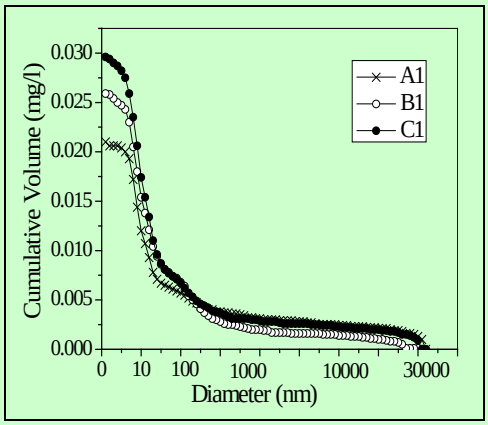

Fig.7 Cumulative pore volume of HDSCs

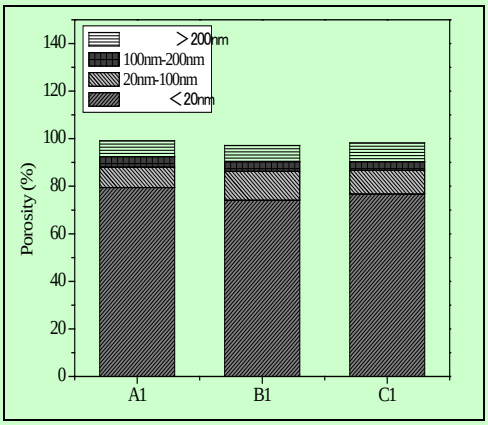

Fig.8 Pore size distribution of HDSCs

Table 5 demonstrates that the porosity, pore volume and specific area of the pores showed an increasing trend with the increase of coating thickness. The average size of pore was below 12.4*nm*. Therefore, the structure of HDSCs was very compact.

Table 5 Pore structure characteristic parameters of HDSCs

	Porosity（%）	Pore Volume（*ml/g*）	Specific Area of Pores（m^2/g）	Average Pore Size（*nm*）
A1	5.0831	0.0210	6.783	12.4
B1	6.1891	0.0259	8.457	12.2
C1	6.9700	0.0296	10.014	11.8

5. Conclusion

(1) HDSCs were designed using an improved DMDA method and Fuller curve. Investigations based on compressive strength, electrical resistivity, sulfate attack and pore structure analysis indicate that the paste thickness on the coated aggregate is a key parameter affecting properties of sulphoaluminate cement concrete.

(2) The compressive strength of HDSCs increased with the increase of paste thickness on the coated aggregates, particularly at the early stages of curing, namely 1 and 3 days. When paste thickness on the coated aggregate was 10μm, the compressive strength increased 23% and 8% compared with 20μm, and increased 37% and 17% compared with 30μm at the curing ages of 1 and 3 days, respectively.

(3) With the increase of paste thickness on the coated aggregates, the electrical resistivity of HDSCs decreased at the same water-binder ratio. When the paste thickness on the coated aggregate was 10μm, the electrical resistivity of HDSC was 44%, 33% and 13% higher than that of sample with 30μm at the ages of 1, 3 and 28 days, respectively.

(4) The sulfate attack resistance coefficients of HDSCs at 28 days were higher than 1.0, suggesting that concrete samples cured in the 5% Na_2SO_4 solutions have much better capability of sulfate attack resistance. With the increase of paste thickness on the coated aggregates, the sulfate attack resistance coefficients decreased evidently. At the same water-binder ratio, the coefficient of HDSCs with 10μm was 10% higher than that of HDSCs with 30μm.

(5) At 28 days, the porosity, pore volume and specific pore area of HDSCs showed an increasing trend with an increasing paste thickness on the coated aggregates. The porosity of HDSCs was below 7% with 70% micropore (<20*nm*), and the average pore size was below 12.4*nm*.

Acknowledge

This work is funded by Natural Science Foundation of China under the grants of 51302104 and 5142109, and the Science and Technology Development Plan of Shangdong Province under the grant of 2014GZX208001. In addition, this work is also sponsored by the Program for Science Research Innovation Team in Colleges by Universities of Shangdong Province.

Reference

[1] Ali M M, Gopal S, Handoo S K. Studies on the formation kinetics of calcium sulphoaluminate. Cement and concrete research. 1994; 24(4): 715-720.

[2] Cheng X, Chang J, Lu L, et al. Study of Ba-bearing sulphoaluminate minerals and cement. Cement and Concrete Composites. 2000; 30(1): 71-81.

[3] Cheng X, Chang J, et al. Study on the Hydration of Ba-bearing calcium sulphoaluminate in the presence of gypsum. Cement and Concrete Research. 2004; 34(11): 2009-2013.

[4] Zhou H, Liu J, et al. Hydration kinetics process of low alkalinity sulphoaluminate cement and its thermodynamical properties. Proc. Eng. 2012; 27: 323-331.

[5] Zhao J, Cai G, et al. Influences of freeze–thaw cycle and curing time on chloride ion penetration resistance of sulphoaluminate cement concrete. Construction and Building Materials. 2014; 53: 305-311.

[6] Duan P, Chen W. Influence of layered double hydroxides on microstructure and carbonation resistance of sulphoaluminate cement concrete. Construction and Building Materials. 2013; 48: 601-609.

[7] Yang C C, Lin J D, Chiang H W, et al. Pore Distribution and Durability of Cement Mortar by the Magnetic Resonance Imaging[C]. Applied Mechanics and Materials. 2015, 764: 132-137.

[8] Zahedi M, Ramezanianpour A A, et al. Evaluation of the mechanical properties and durability of cement mortars containing nanosilica and rice husk ash under chloride ion penetration. Construction and Building Materials. 2015; 78: 354-361.

[9] Hang M, Li H. Pore structure and chloride permeability of concrete containing nano-particles for pavement. Construction and Building Materials. 2011; 25(2): 608-616.

[10] Hwang C L, Hsieh S L. The effect of fly ash/slag on the property of reactive powder mortar designed by using Fuller's ideal curve and error function. Computers and Concrete. 2007; 4(6): 425-436.

[11] Hwang C L, Chen C.T. Application of Fuller's ideal curve and error function to making high performance concrete using rice husk ash. Computers and Concrete. 2012; 10(6): 1123-1126.

[12] Hwang C L, S.L Lee et al. The study on the densified mixture design method of high performance concrete and its early properties. Journal of the Chinese Hydraulic Engineering. 1996; 8(2): 207-219.

[13] Chen Y Y, Tuan B L, et al. Effect of paste amount on the properties of self-consolidating concrete containing fly ash and slag. Construction and Building Materials. 2013; 47: 340-346.

[14] Hwang C L, Huynh T P. Investigation into the use of unground rice husk ash to produce eco-friendly construction bricks. Construction and Building Materials. 2015; 93: 335-341.

[15] Wang H Y, Tsai K C. Engineering properties of lightweight aggregate concrete made from dredged silt. Cement and Concrete Composites. 2006; 28(5): 481-485.

[16] Chang P K. An approach to optimizing mix design for properties of high-performance concrete. Cement and Concrete Research. 2004; 34(4): 623-629.

[17] Felekog˘lu B, Türkel S, Baradan B. Effect of water/cement ratio on the fresh and hardened properties of self-compacting concrete. Building Environment. 2007; 42(4): 1795-802.

[18] Aitcin P C. The durability characteristics of high performance concrete: a review. Cement and Concrete Composites. 2003; 25(4-5): 409-20.

[19] Wang H Y, Hwang C L. An approach of using ideal grading curve and coating paste thickness to evaluate the performances of concrete-(1): Theory and formulation. Computers and concrete. 2012; 10(10): 19-33.

[20] Okundi E, Buenfeld N R, et al. Effect of cement content on transport in concrete. Magazine of Concrete Research, 1998, 50(4):339-351.

[21] Hwang C L, Lee S L, Lin F Y, et al. Densified mix design algorithm and early properties of HPC. J. Chin. Inst. Civil Hydraul. Eng, 1994; 8(2): 217-219.

[22] Kolias S, Georgiou C. The effect of paste volume and of water content on the strength and water absorption of concrete. Cement and Concrete Composites. 2005; 27(2): 211-216.

[23] Chen Y, Wei J, Li F, et al. Effect of the paste coating layer and mortar coating layer on the properties of fresh self-compacting concrete. Journal of Sustainable Cement-Based Materials, 2015; 4(3): 194-204.

[24] Sobolev K, Amirjanov A. Application of genetic algorithm for modeling of dense packing of concrete aggregates. Construction and Building Materials. 2010; 24(8): 1449-1455.

[25] Gonzalez C, Etxeberria M. Properties of high performance concrete made with recycled fine ceramic and coarse mixed aggregates. Construction and Building Materials. 2014; 68: 618-626.

[26] Elrahman M A. Hillemeier B. Combined effect of fine fly ash and packing density on the properties of high performance concrete: An experimental approach. Construction and Building Materials. 2014; 58: 225-233.

[27] Bai W, Zhang J. Proportion design of polymeric cement concrete based on volumetric analysis. Applied Mechanics and Materials. 2014; 584: 1809-1813.

[28] García-Taengua E, Sonebi M, Crossett P, et al. Performance of sustainable SCC mixes with mineral additions for use in precast concrete industry. Journal of Sustainable Cement-Based Materials. 2015; 1-19.

[29] Zhang J, Wang S, Lu L. Effect of aggregate gradation with Fuller distribution on properties of sulphoaluminate cement concrete. Journal of Wuhan University of Technology-Mater. 2015; 30(5): 1029-1035.

[30] GB/T50080-2002. Standard for test method of performance on ordinary fresh concrete. Beijing: Standardization Administration of the People’s Republic of China; 2002.

[31] GB/T 50081-2002. Standard for test method of mechanical properties on ordinary concrete. Beijing: Standardization Administration of the People's Republic of China; 2002.

[32] GB/T 50082-2009. Standard for test method of long-term performance and durability of ordinary concrete. Beijing: Standardization Administration of the People's Republic of China; 2009.

[33] Hüsken G, Brouwers H J H. A new mix design concept for earth-moist concrete: A theoretical and experimental study. Cement and Concrete Research. 2008; 38(10): 1246-1259.

[34] W B Fuller, S E Thompson. The laws of proportioning concrete. J. Transp. Eng.-ASCE. Cement and Concrete Composites 1907; 59: 67-143.

[35] Cai Z, Huang Z et al. New approach to design concrete mix proportions by coating thickness of aggregates. Journal of Building Materials. 2009; 12(4): 152-157.

[36] Zhang J, Huang Z et al. Effects of paste thickness on coated aggregates on properties of concrete. Journal of Building Materials. 2009; 12(4): 384-427.

[37] Nili M, Ehsani A. Investigating the effect of the cement paste and transition zone on strength development of concrete containing nanosilica and silica fume. Materials & Design. 2015; 75: 174-183.

[38] Poon C S, Shui Z H, Lam L. Effect of microstructure of ITZ on compressive strength of concrete prepared with recycled aggregates. Construction and Building Materials. 2004; 18(6): 461-468.

[39] Medeiros-Junior R A, Lima M G. Electrical resistivity of unsaturated concrete using different types of cement. Construction and Building Materials, 2016; 107(15): 11-16.

[40] Ghods P, Isgor O B, Pour-Ghaz M. A practical method for calculating the corrosion rate of uniformly depassivated reinforcing bars in concrete. Materials and Corrosion. 2007; 58(4): 265-272.

[41] Liu Z, Zhang Y, Jiang Q. Continuous tracking of the relationship between resistivity and pore structure of cement pastes. Construction and Building

457 Materials. 2014; 53(28): 26-31.
458 [42] Wang Z, Zeng Q, Wang L, et al. Characterizing blended cement pastes under
459 cyclic freeze–thaw actions by electrical resistivity. Construction and Building
460 Materials. 2013; 44: 477-486.
461 [43] Su N, Hsu K C, Chai H W. A simple mix design method for self-compacting
462 concrete. Cement and Concrete Research, 2001; 31(12): 1799-1807.